

# Spray-drying process for synthesis of nanosized $\text{LiMn}_2\text{O}_4$ cathode

H. M. WU, J. P. TU\*, Y. Z. YANG, D. Q. SHI

Department of Materials Science and Engineering, Zhejiang University, Hangzhou 310027, People's Republic of China

E-mail: [tujp@cmsce.zju.edu.cn](mailto:tujp@cmsce.zju.edu.cn)

Published online: 15 May 2006

Nanosized  $\text{LiMn}_2\text{O}_4$  cathode material was synthesized by a spray-drying process. The calcined  $\text{LiMn}_2\text{O}_4$  powder retained a well-define spinel structure and good crystallization. Electrochemical measurements showed that the nanosized  $\text{LiMn}_2\text{O}_4$  reached an initial discharge capacity of  $131 \text{ mAh}\cdot\text{g}^{-1}$  at 1/5 C rate and exhibited a good cycling property at 1 C rate. The results indicate that spray-drying method is a promising method suitable for mass production of nanosized  $\text{LiMn}_2\text{O}_4$  with improved electrochemical performances and low cost. © 2006 Springer Science + Business Media, Inc.

## 1. Introduction

Lithium ion secondary batteries are now the prevailing rechargeable batteries due to their high working voltage and high-energy density. Commercial lithium ion batteries use  $\text{LiCoO}_2$  and graphite as cathode and anode materials, respectively [1]. Further developments of large-sized lithium ion batteries are strongly required for electric vehicles (EV). So the higher performance of the electrode material in terms of safety, environment friendliness, and cost are to be expected [2]. Now, in these respects, lithium manganese oxides ( $\text{LiMn}_2\text{O}_4$ ) have been extensively investigated to substitute  $\text{LiCoO}_2$  positive electrodes in terms of their cost, abundance, safety and non-toxicity [3–5].

For the future application in EV, Lithium ion secondary batteries required excellent electrochemical ability, which especially could be charged and discharged with a high current density quickly. It is believed that single-phase, homogeneity, uniform particle morphology, and large surface area are considered as desired characters in order to achieve better electrode properties [6]. Recently, it is reported [7] that nanostructured  $\text{LiMn}_2\text{O}_4$  have a higher rate capability than those reported for the spinel  $\text{LiMn}_2\text{O}_4$  prepared by conventional solid-state reactions [8, 9].

In this work, nanosized  $\text{LiMn}_2\text{O}_4$  cathode material has also been synthesized successfully by a novel spray-drying process. In contrast, the conventional solid-state reactions [10], sol-gel [11] and Pechini [12] processes often involve a long processing time at high temperatures to form the required crystalline phases, moreover, the final product usually contains the impurity phases, irregular

morphology, larger particle size and broader particle size distribution. Via spray-drying process, the sintering time is reduced heavily, and this method can provide good control on the crystalline growth, compositional homogeneity, morphology and microstructure.

## 2. Experimental

Nanosized  $\text{LiMn}_2\text{O}_4$  cathode was prepared by a spray-drying method. Stoichiometric amounts of  $\text{CH}_3\text{COOLi}\cdot 2\text{H}_2\text{O}$  (A. R.) and  $\text{Mn}(\text{CH}_3\text{COO})_2\cdot 4\text{H}_2\text{O}$  (A. R.) were dissolved in distilled water, and then via a spray-dryer, the resulting solution was dried to form a mixture of precursor by first atomizing via a sprinkler at an air pressure of 0.2 MPa, and then spray-drying by hot air with the inlet temperature at  $220^\circ\text{C}$ , and the exit air temperature at  $110^\circ\text{C}$ . The as-prepared precursor powders were calcined at  $500^\circ\text{C}$  for 6 h in air, and then elevated the temperature to  $750^\circ\text{C}$  for 5 h with intermittent grindings. The calcining time at high temperature is shorted a lots [13], which decreased the average particle size of  $\text{LiMn}_2\text{O}_4$  powders to the order of nanometers. The phase structure of the powder was analyzed by X-ray diffraction (XRD) on a Rigaku D/max-rA diffractometer with  $\text{Cu K}\alpha$  radiation using a  $2\theta$  step of  $0.02^\circ$ . The powder morphology was observed by a field emission scan electron microscopy (FESEM, FEI SIRION JY/T010-1996) and a transmission electron microscope (TEM, JEM-2010).

For electrochemical measurements, the mixture of  $\text{LiMn}_2\text{O}_4$  powders, acetylene carbon black, and

\* Author to whom all correspondence should be addressed.

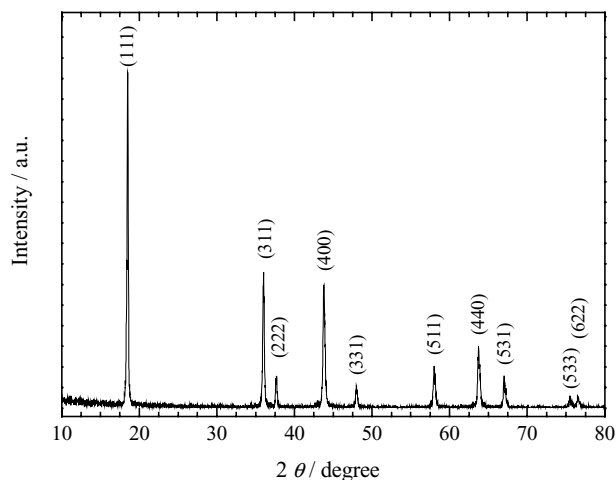


Figure 1 XRD pattern of nanosized  $\text{LiMn}_2\text{O}_4$  powder.

polyvinylidene fluoride (PVDF) with a weight ratio of 80:10:10 was used as the cathode, and assembled into the coin-type cells (CR 2025) in an Ar-filled glove box. The metallic lithium foil was used as anode, 1 M  $\text{LiPF}_6$  in ethylene carbonate (EC)-dimethyl carbonate (DME; 1:1 in volume) as the electrolyte solution, and a polypropylene (PP) microporous film (Cellgard 2300) as the separator. The galvanostatic charge-discharge tests were conducted on a PCBT-138-8D-A battery program-control test system with the cut-off voltages of 3.2 V and 4.3 V (versus  $\text{Li}/\text{Li}^+$ ) under a specific current density (a nominal specific capacity of  $120 \text{ mAh g}^{-1}$  was assumed to convert the current density into C rate). The cyclic voltammogram (CV) tests were performed on a CHI660A electrochemical workstation at room temperature.

### 3. Results and discussion

Fig. 1 shows the XRD patterns of the obtained  $\text{LiMn}_2\text{O}_4$  powders. All peaks can be indexed as pure and well-crystallized  $\text{LiMn}_2\text{O}_4$  phase with an ordered spinel structure and a space group of  $Fd-3m$ . The lattice parameters calculated by the XRD data (Fig. 1) of the spinel structure material is  $a_0 = 8.2531 \text{ \AA}$ , which is very close to the standard data ( $a_0 = 8.247 \text{ \AA}$ ) given by JCPDS 35-0782. These XRD results demonstrate that the spray-drying process developed in the present work could synthesize single-phased product  $\text{LiMn}_2\text{O}_4$  with no unwanted impurity phases, such as  $\text{Mn}_2\text{O}_3$  and  $\text{LiMn}_2\text{O}_3$  compounds [14].

Typical powder morphologies of spinel  $\text{LiMn}_2\text{O}_4$  are shown in Fig. 2. The  $\text{LiMn}_2\text{O}_4$  particles have an average size of about 100 nm and show uniform particles and particle size distribution in Fig. 2a. It is obviously observed that the conglomeration took place among some particles. From the TEM image (Fig. 2b), interference fringes are observed on fine particles. This suggests that they are in a good crystalline state.

In order to evaluate the electrochemical properties of nanosized  $\text{LiMn}_2\text{O}_4$  prepared by spray-drying method

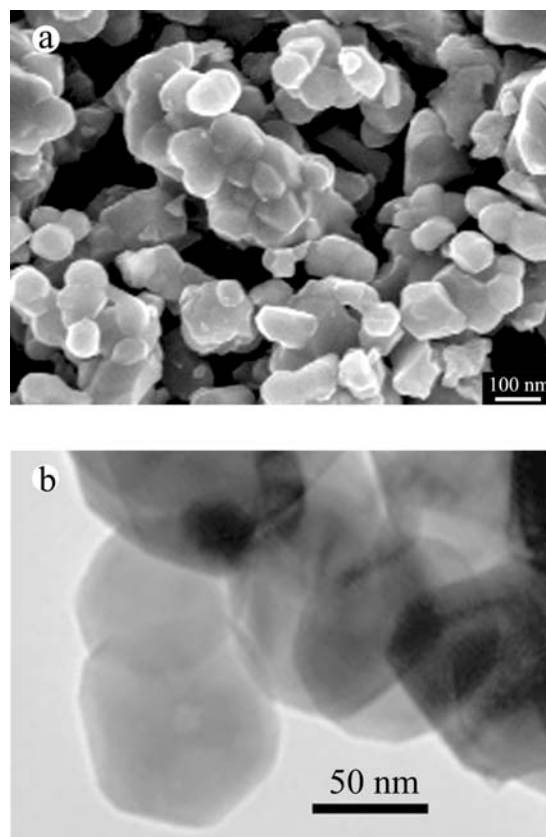


Figure 2 Powder morphology of nanosized  $\text{LiMn}_2\text{O}_4$  a: SEM image; b: TEM image.

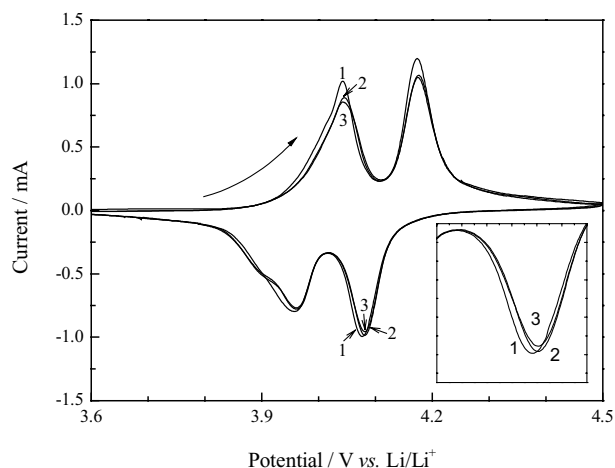


Figure 3 Consecutive cyclic voltammograms of nanosized  $\text{LiMn}_2\text{O}_4$  at a scan rate of  $0.1 \text{ mV s}^{-1}$ . Cycle numbers are indicated.

during the electrochemical lithium insertion/extraction, a variety of electrochemical tests were performed. The typical first three cyclic voltammograms of the compound at a scan rate of  $0.1 \text{ mV s}^{-1}$  are shown in Fig. 3. The initial charge-discharge behaviors of  $\text{LiMn}_2\text{O}_4$  compound tested galvanostatically at the charge and discharge rate ( $1/5 \text{ C}$ ) between 3.2 V and 4.3 V are shown in Fig. 4.

As seen in Fig. 3, the first three cyclic voltammograms scanned at  $0.1 \text{ mV s}^{-1}$  show two sharp couples of

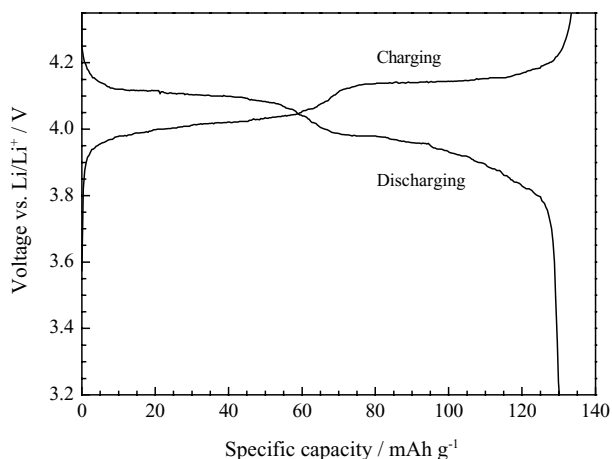


Figure 4 Initial charge/discharge curves of nanosized  $\text{LiMn}_2\text{O}_4$  at 1/5 C rate between 3.2 V and 4.3 V.

redox peaks (4.04/3.96 V and 4.17/4.08 V), which is the characteristic of spinel  $\text{LiMn}_2\text{O}_4$ . The two couples of redox peaks indicate that the lithium insertion/extraction in nanosized  $\text{LiMn}_2\text{O}_4$  are reversible. Consecutive cycling causes a little change between the first cycle and the second in the shape of the curves. But between the second and third cycle, the shape of the curves has no visible change. During the first two cycles, the curve change is due to the SEI forming, but at the next cycling process, the SEI is stable and so the shape of the curves has no visible change.

Fig. 4 shows that the initial charge and discharge specific capacities of nanosized  $\text{LiMn}_2\text{O}_4$  are determined to be 134 and 131  $\text{mAh g}^{-1}$  (corresponding to 88% of the theoretical capacity of 148  $\text{mAh g}^{-1}$ ), respectively, indicating a coulombic efficiency reaches 98%. It can be seen that two distinct plateaus appeared on charge curve as well as on discharge curve. For charging process, they locate at the potentials about 4.00 V and 4.16 V, respectively, but for the discharging process, they locate at 4.00 V and 3.90 V. The two plateaus correspond to the two pairs of redox current peaks in cyclic voltammogram curves in Fig. 3, suggesting that both the intercalation and deintercalation of lithium ion are carried out in two steps.

The specific discharge capacity in a potential range 3.2 V–4.3 V versus cycle number is presented in Fig. 5. For the first three cycles the cell was cycled at 1/5 C rate, then the rate was increased to 1 C. When altering the lower rate to high rate, the discharge capacities decrease heavily. At 1/5 C rate, the value of capacity is about 130  $\text{mAh g}^{-1}$ , but at 1C rate, it is about 120  $\text{mAh g}^{-1}$ . With increasing the cycle times at 1 C rate, the capacity decreases slowly. Till to 50th, the capacity still maintains a value of 112  $\text{mAh g}^{-1}$ . It shows that the discharge capacity retention is about 85% of the initial capacity of 1/5 C rate, and it only fades 8  $\text{mAh g}^{-1}$  of the first capacity of 1 C rate. But ordinary  $\text{LiMn}_2\text{O}_4$  is only about 100  $\text{mAh g}^{-1}$

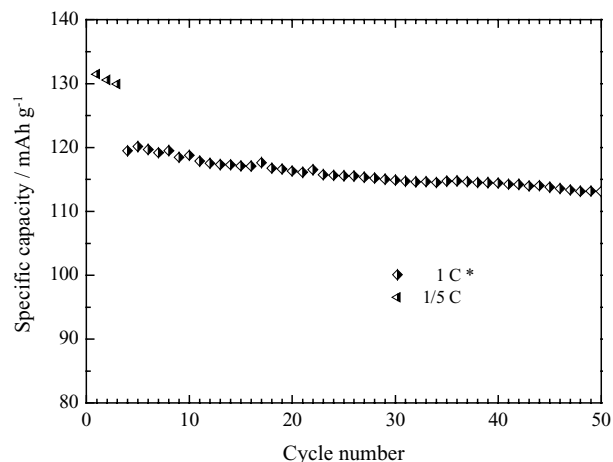


Figure 5 Cycling stability curve of nanosized  $\text{LiMn}_2\text{O}_4$  at the range of 3.2 V–4.3 V \* 1/5 C rate in first three cycles and 1 C rate in the following cycles.

after cycled 50 cycles [15]. These results indicate that the nanosized  $\text{LiMn}_2\text{O}_4$  has excellent cycle stability.

#### 4. Conclusions

In summary, the spray-drying process followed a short time calcination has successfully synthesized nanosized spinel  $\text{LiMn}_2\text{O}_4$ . The calcined powder retained a well-defined spinel structure and good crystallization without any impurity. Special capacity of 131  $\text{mAh g}^{-1}$  is obtained when they are measured at 1/5 C rate between 3.2–4.3 V. At high rate (1C), the nanosized material still exhibits excellent cycle property. The spray-drying process appears to be an attractive method for fabrication of cost-effective nanosized electrode material for lithium ion secondary batteries.

#### References

1. K. OZAWA, *Solid State Ion.* **69** (1994) 212.
2. T. HORIBA, K. HIRONAKA, T. MATSUMURA, T. KAI, M. KOSEKI and Y. MURANAKA, *J. Power Sources* **119–121** (2003) 893.
3. D. GUYOMARD and J. M. TARASCON, *J. Electrochem. Soc.* **139** (1992) 937.
4. Y. XIA, Y. ZHOU and M. YOSHIO, *J. Electrochem. Soc.* **144** (1997) 2593.
5. Y. Y. XIA, N. KUMADA, and M. YOSHIO, *J. Power Sources* **90** (2000) 135.
6. Y. M. HON, S. P. LIN, K. Z. FUNG and M. H. HON, *J. Eur. Ceram. Soc.* **22** (2002) 653.
7. Y. ZHANG, H. C. SHIN, J. DONG, and M. L. LIU, *Solid State Ion.* **171** (2004) 25.
8. C. Y. WAN, Y. NULI, J. ZHUANG, and Z. JIANG, *Mater. Lett.* **56** (2002) 357.
9. M. R. PALACIN, G. ROUSSE, M. MORCRETTE, L. DUPONT, C. MASQUELIER, Y. CHABRE, M. HERVIEU and J. M. TARASCON, *J. Power Sources* **97/98** (2001) 398.
10. J. SUGIYAMA, T. ATSUMI, T. HIOKI, S. NODA and N. KAMEGASHIRA, *J. Alloys Comp.* **235** (1996) 163.

11. W. LIU, K. KOWAL and G. C. FARRINGTON, *J. Electrochem. Soc.* **143** (1996) 3590.
12. W. LIU, G. C. FARRINGTON, F. CHAPUT and B. DUNN, *J. Electrochem. Soc.* **143** (1996) 879.
13. H. M. WU, J. P. TU, Y. F. YUAN, Y. LI, X. B. ZHAO and G. S. CAO, *Scripta Mater.* **52** (2005) 513.
14. D. I. SIAPKAS, C. L. MITSAS, I. SAMARAS, T. T. ZORDA, G. MOUMOZIAS, D. TERZIDIS, E. HATZIKRANIOTIS, S. KOKKOU, A. VOULGAROPOULOS and K. M. PARASKEVOPOULOS, *J. Power Sources* **72** (1998) 22.
15. Y. SUN, Z. WANG, L. CHEN and X. HUANG, *J. Electrochem. Soc.* **150** (2003) A1294.

*Received 10 June  
and accepted 8 August 2005*